A technique for atmospheric measurements of stable carbon isotope ratios of isoprene, methacrolein, and methyl vinyl ketone

R. Iannone • R. Koppmann • J. Rudolph

Abstract A technique was developed to measure stable carbon isotope ratios ($^{13}C/^{12}C$) of light volatile organic compounds (VOCs) such as isoprene, methacrolein (MACR) and methyl vinyl ketone (MVK) using gas chromatography combustion isotope ratio mass spectrometry (GCC-IRMS). An automated sampling and cryofocussing system allowed for the extraction of VOCs from air samples of up to 140 L of air collected over 3 h, and the subsequent $^{13}C/^{12}C$ analysis of the VOCs by GCC-IRMS. Chromatography using selective transfer between two columns was used to improve the separation for selected compounds, increasing peak resolution and attaining less noisy baselines. Still, some target compounds could not be completely separated from co-eluting peaks. To reduce the bias of isotope ratio determinations, which can result from incomplete peak resolution, a peak-fitting procedure has been developed. In cases of overlapping peaks or substantial baseline drift, this peak fitting allows more accurate determination of isotope ratios than conventional integration schemes. Comparisons between off-line IRMS measurements and a peak-evaluation procedure using a prepared VOC gas-phase standard show that isotope ratios derived from large (>1 ng of carbon per peak) and well-resolved peaks have a reproducibility of ±0.3‰. With smaller masses in the range of 0.1–1 ng of carbon, reproducibility decreased to ±(0.5–0.8)‰. For a 140 L sample of air, such small masses of carbon correspond to mixing ratios in the low pptV range. The developed measurement technique was applied to a small set of ambient air samples taken during hot, sunny periods from late May to early August, 2005, at Forschungszentrum Jülich, Germany, a semi-rural area. The range of $\delta^{13}C$ values determined for isoprene, benzene, and toluene are consistent with those reported in the literature. GCC-IRMS results of $\delta^{13}C$ for ambient samples of isoprene, MACR, and MVK, measured at mixing ratios of 15–280 pptV, are presented and discussed.

Keywords Stable isotope ratios · GC-IRMS · Isoprene · Methacrolein · Methyl vinyl ketone

1 Introduction

Volatile organic compounds (VOCs) have been subjects for studies of their emissions and their atmospheric removal due to oxidation via OH radicals, O_3, NO_3 radicals and Cl atoms; reviews can be found in Kesselmeier and Staudt (1999), Atkinson (1997, 2000), and Atkinson and Arey (1998, 2003). Isoprene has a global biogenic production in the range of 350–500 (Tg C)/yr (Guenther et al. 1995; Poisson et al. 2000; Levis et al. 2003) and has a large impact on atmospheric processes. It can affect the oxidative state of large air masses (Poisson et al. 2000; Monson and Holland 2001) and is an important precursor for O_3. Recent evidence suggests that isoprene may contribute toward the formation of secondary organic aerosols through photooxidation with OH radicals (Claeys et al. 2004). The main products of isoprene oxidation via OH radicals and O_3 are methacrolein (MACR) and methyl vinyl ketone (MVK).

Concentration measurements of VOCs have been developed over several decades and tropospheric measurements of isoprene, MACR, and MVK have been reported by several groups. Following the first measurements of MACR and MVK in the atmosphere (Pierotti et al. 1990), several field studies investigated the relationships between isoprene, MACR and MVK (Montzka et al. 1995; Biesenthal et al. 1997; Stroud et al. 2001; Warneke et al. 2001; Wiedinmyer et al. 2001; Apel et al. 2002). Komenda et al. (2003) have presented an on-line system for measurements at mixing ratios of some tens of pptV, and Lee et al. (1998) reported on the use of a 2,4-dinitrophenylhydrazine (2,4-DNPH) derivatization method for soluble carbonyl products of isoprene oxidation.

Though concentration measurements are essential, it is difficult to study the kinetics of isoprene oxidation in real atmospheres with concentration measurements alone. Isotopic fractionation is a useful approach for studying isoprene oxidation kinetics. Several studies of the stable carbon isotopic fractionation of non-methane hydrocarbons (NMHCs) in tropospheric samples using gas-chromatography combustion isotope ratio mass spectrometry (GCC-IRMS) (Rudolph et al. 1997; Tsunogai et al. 1999; Rudolph et al. 2000; Saito et al. 2002) aided in the interpretation of the sources and sinks of the studied NMHCs. The development of the Isotopic Hydrocarbon Clock concept (Rudolph and Czuba 2000), an extension of the Hydrocarbon Clock method (McKeen and Liu 1993), provided the theoretical framework.

Notwithstanding the recent development of GCC-IRMS techniques for the $\delta^{13}C$ determination of tropospheric NMHCs, very few reports have been made of such measurements for volatile organic compounds (VOCs) at very low mixing ratios (i.e. several pptV) (Bill et al. 2002, 2004; Komatsu et al. 2005). One study describes the use of 2,4-DNPH derivatization for the GCC-IRMS analysis of formaldehyde and acetaldehyde to determine $\delta^{13}C$ values. However, this methodology has not yet been used for MACR or MVK. The derivatization reaction can result in a change of isotope ratios due to fractionation effects and the addition of carbon atoms with different isotope ratios. Although it is possible to correct for these effects, such a correction is an additional source of uncertainty. Thus, in this work, a method was developed which does not require derivatization.

A large volume of air is required for the GCC-IRMS analysis of VOCs such as isoprene, MACR and MVK. This is due to the low natural abundance of ^{13}C isotopes, the low mixing ratios of the targeted VOCs (i.e. low pptV to few ppbV range), and the necessity to determine carbon isotope ratios with per mille or better accuracy. Thus, depending on mixing ratios, a sample size of some tens to hundreds of liters of air is required for GCC-IRMS measurement of stable-carbon isotope ratios in atmospheric VOCs. Another requirement is that for GCC-IRMS analyses better peak resolution than for concentration measurements is required. Improved peak separation, particularly amongst the hundreds of VOC peaks in ambient samples, is extremely valuable to reduce bias in peak evaluation. Also, to some extent, peak-fitting techniques can be used to reduce bias in δ^{13}C values determined for overlapping peaks.

In this paper, we present a GCC-IRMS technique that can accurately determine the stable carbon isotope ratios of isoprene, MACR, and MVK. Although the method was developed primarily for measurements of these compounds, the technique also allows for measurements of other VOCs. In this study, the δ^{13}C values of *n*-pentane, benzene and toluene in ambient air samples were also analyzed. This technique involves the concentration of VOCs and the removal of water for ambient air samples of 140 L volume. This technique is an extension of previous methods (e.g. Rudolph et al. 2000; Anderson et al. 2003). The method was tested by analyzing a small set of atmospheric samples obtained from late May to early August, 2005.

2 Experiment

The system consisted of several components: (1) a three step cryofocussing system (Online TDS G Large; Gerstel GmbH & Co. KG, Mülheim an der Ruhr, Germany), (2) an Agilent 6890 Gas Chromatograph equipped with both a 60 m×5 μm film×0.32 mm ID DB-1 column (Agilent Technologies) and a 50 m×1.8 μm film×0.32 mm ID BP624 column (SGE Scientific), (3) a furnace interface, and (4) an Isoprime Isotope Ratio Mass Spectrometer (IRMS) (GV Instruments, Manchester, UK). Figure 1 provides an overall schematic of the system.

2.1 Cryofocussing system

The cryofocussing system used in this study was custom built to allow for the concentration of trace gases from sample volumes in the range of several hundred liters (at standard temperature and pressure). It was comprised of four unpacked traps (Traps I–IV), three pneumatic switching valves, two cryotraps, and a capillary trap. The switching valves and the bulk of the transfer lines were contained within an enclosure which was held at a constant temperature of 393 K. Cryotrap I and Traps I–IV were positioned outside of the enclosure and transfer lines were individually maintained at 393 K through electrical heating.

Traps I–IV were used to remove water from atmospheric samples at 233 K, following the procedure suggested by Thompson (2003). For a 140 L air sample, several mL of water were trapped during sample collection. Traps I–IV did not contain any absorptive packings in order to avoid possible sample contamination and to minimize flow resistance. Cryotrap I was packed with spherical porous silica beads (Unibeads 3S, 60/80, 100 Å pore size, Alltech) and Cryotrap II was packed with glass beads (80/100, Alltech). The Capillary Trap was located at the top of the DB-1 column inside the GC oven; it allowed for the cooling of a 5 cm length of the capillary. Temperatures for each trap were individually controlled by a combination of cooling by liquid nitrogen and electrical heating. Table 1 provides a summary of the dimensions and flow rates through the traps during sample collection. Inlet sample flow was

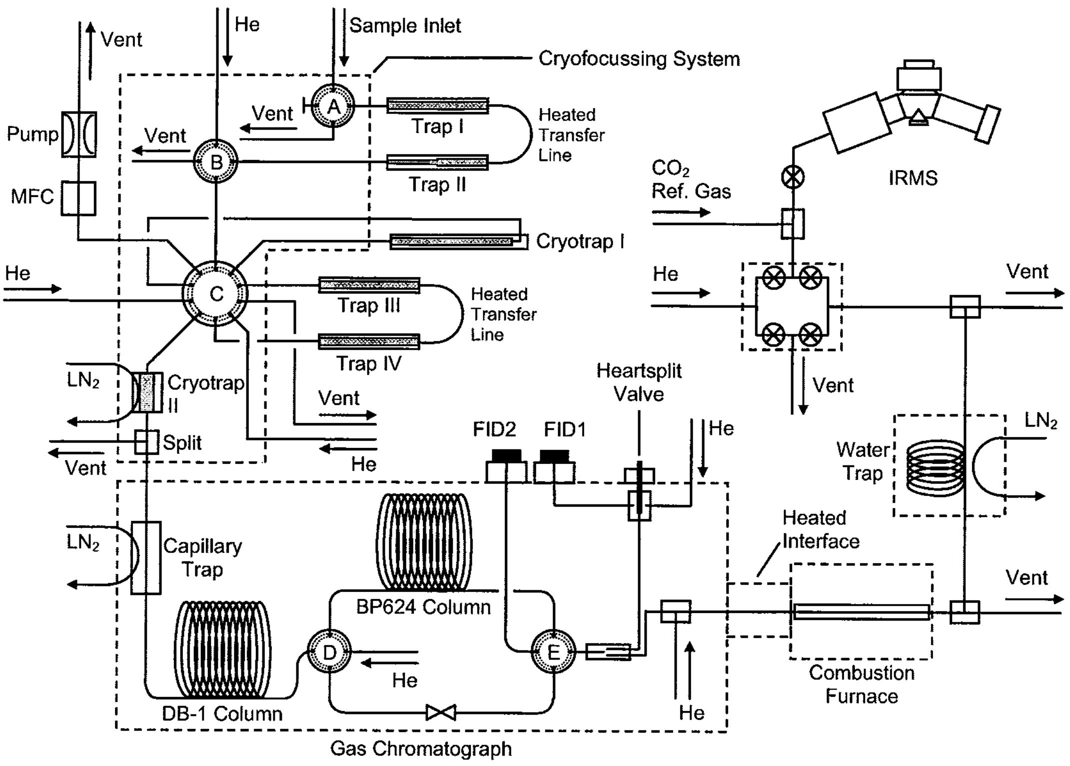

Fig. 1 Schematic of the GCC-IRMS system for measurements of the stable carbon isotope ratios of ambient VOCs. *Broken lines* indicate temperature controlled enclosures for separate instrument components

controlled using an external pump coupled with a mass flow controller. A control box allowed the setting of a wide range of experimental parameters such as temperatures, and valve switching as function of time.

Two main valve configurations were used during the procedure: (1) Sampling Mode and (2) Transfer Mode (both depicted in Fig. 2). In Sampling Mode, the sample air was drawn at 800 mL min^{-1} through the cooled Traps I and II (both at 233 K), and through the cooled adsorption tube of Cryotrap I (123 K). The removal of water by traps at sub-ambient temperature is very similar to the procedure used by Apel et al. (2002) for concentration measurements of a wide range of VOC, including isoprene, MVK and MACR. In the study of Apel et al. it was shown that there were no losses of isoprene, MACR, and MVK over a relative

Table 1 Dimensions and flow rates of the traps comprising the cryofocussing system during the collection of large atmospheric volumes of air

Trap	Length, mm	I.D., mm	Volume, cm^3	Adsorption flow rate, mL min^{-1}	Desorption flow rate, mL min^{-1}
Trap I	498	28	219	850	75
Trap II	210	18	59.4	850	75
Trap III	108	5	8.48	60	100
Trap IV	108	5	8.48	60	100
Cryotrap I	300	11	61.3	850	100
Cryotrap II	108	5	8.48	60	2.7[a]
Capillary Trap	50	–	–	2.7[a]	2.7[a]

[a] He carrier gas flow rates.

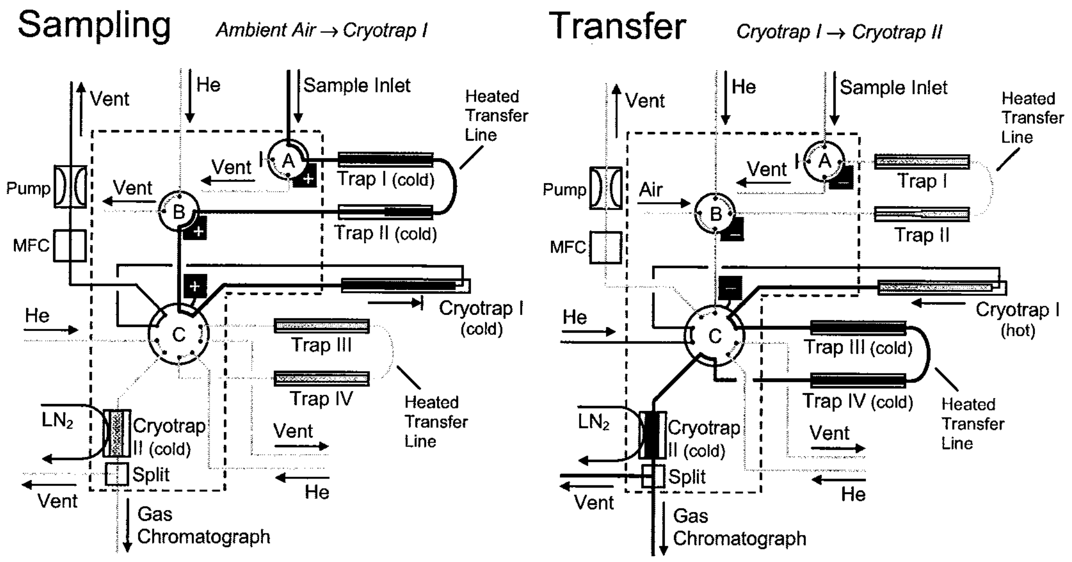

Fig. 2 Valve positions for sampling and GC injection modes for the cryofocussing system. *Thick lines* indicate path of sample flow, *grey lines* indicate other flows, and the *broken line* represents the enclosure. The split prior to Cryotrap II is open during VOC desorption at Cryotrap I (sample transfer to Cryotrap II) and kept closed at all other times

humidity range of 5–95%. Similar results were reported by Bandowe (2005). VOCs were adsorbed onto the packings within the Cryotrap I tube and the sample air was vented. Upon changing to Transfer Mode 3 h later, Cryotrap I was heated to 473 K at a rate of 60 K min^{-1} and the desorbed VOCs were then transferred, via a stream of helium at 100 mL min^{-1}, to Cryotrap II which during transfer was cooled to 163 K. Here, the sample VOCs were again adsorbed onto glass beads and the helium was vented. After a 2 min period, Cryotrap II was rapidly heated to 523 K, the desorbed VOCs were injected onto the GC column of the gas chromatograph, and the GC temperature program was remotely started. The Capillary Trap at the top of the GC column, inside the oven, focused the VOCs on the column at 213 K for 5 min to attain a narrow injection profile. This trap was then heated to 523 K at a rate of 50 K min^{-1}, allowing the VOCs to undergo GC separation. Figure 3 provides an annotated example of a sequence of events for the sampling and injection of a 140 L air sample.

2.2 Gas chromatographic separation

The VOCs were separated using a partial two-dimensional gas chromatography technique. VOCs separated on a non-polar DB-1 column (60 m×5 μm film× 0.32 mm ID) could be sent to a polar BP624 column (50 m×1.8 μm film×0.32 mm ID) for additional separation during a single measurement. The GC was configured for selective transfer through the use of two four-way switching valves. Valve switching was programmed as a time series.

Two valve configurations used here are shown in Fig. 4 and these correspond to the following sample flow paths: (1) sample→FID2 and (2) sample→IRMS. In the sample→FID2 mode, separation occurs on the DB-1 column and eluting VOCs are sent to FID2. In the sample→IRMS mode, VOCs eluting from the DB-1 column underwent an additional separation on the BP624 column and then entered the combustion furnace.

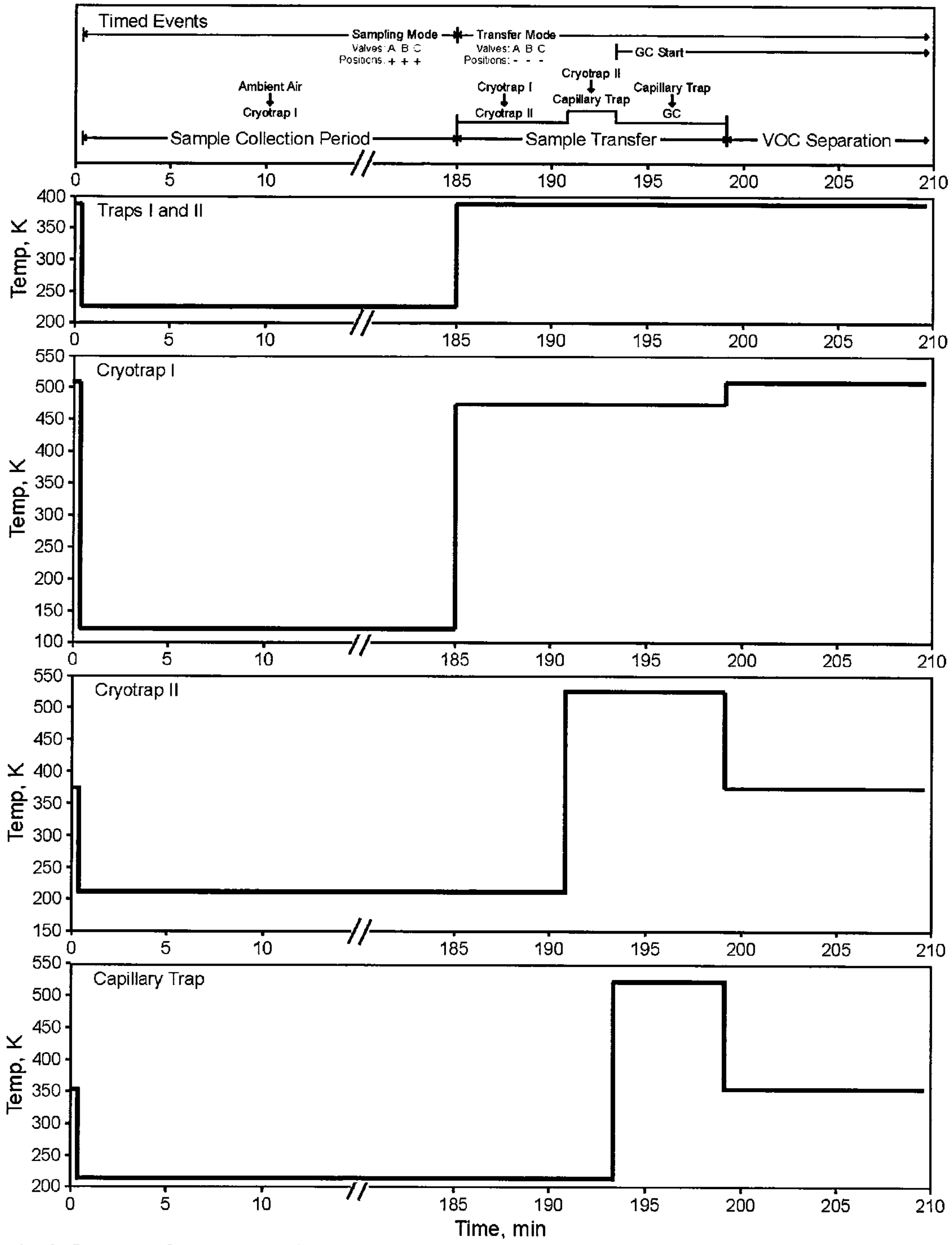

Fig. 3 Program of temperature changes, valve-position changes, and other timed events for the enrichment and transfer of a 140 L air sample in the cryofocussing system

2.3 The GC-IRMS interface

The separated VOCs exiting the GC flowed through a commercially available (GV Instruments) combustion interface. This consisted of a quartz tube partially held in a heated zone of 523 K and, further downstream, within a furnace held at 1123 K. The portion of quartz tube within the combustion furnace was packed with CuO particles (0.1–0.5 mm), which cause the quantitative combustion of VOCs to CO_2 and H_2O.

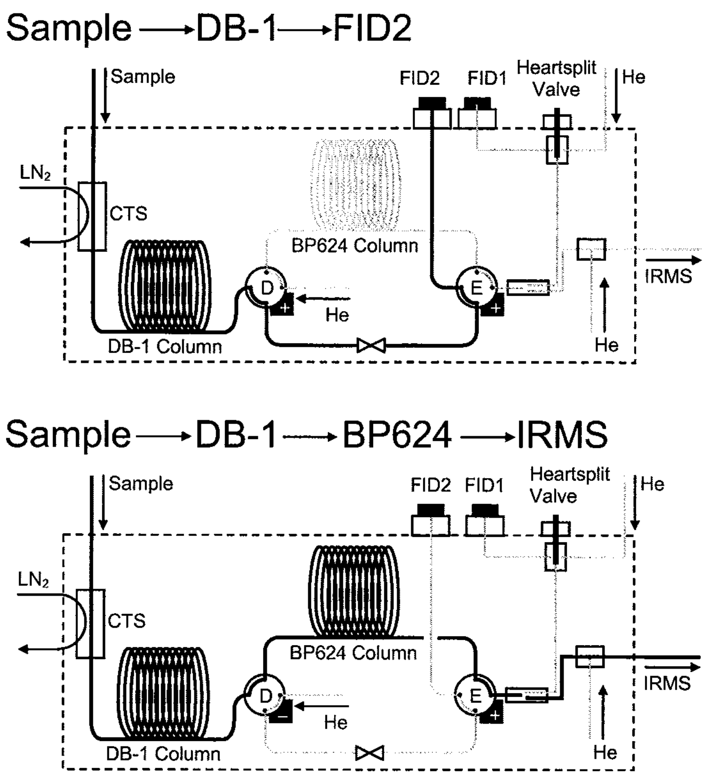

Fig. 4 Valve positions for two-dimensional chromatography. *Black lines* indicate path of sample flow and *grey lines* indicate other flows. The Sample→DB-1→FID2 configuration is the standard setup for initiating GC runs whereby compounds are separated on the DB-1 column and are eluted to FID2. Compounds of interest for isotopic composition are diverted to the BP624 column by switching the position of *Valve D* (*Valve E* always remains in the + position); this is the Sample→DB-1→BP624→IRMS configuration. After eluting from the BP624 column, sample compounds proceed toward the IRMS. The Heartsplit valve always remains closed

After conversion to CO_2 and water, the gas flow then passed through a cold trap which consisted of a coiled capillary maintained at 173 K by a combination of cooling with liquid nitrogen and electrical heating. The cold trap removed the water generated from the combustion process. The trap was regenerated every night by heating it to 323 K.

2.4 Mass spectrometry

The $^{12}CO_2/^{13}CO_2$ gas stream entered the source of the Isoprime IRMS (GV Instruments, Manchester, UK) through an open split. The three ion beams comprising *m/z* 44, 45, and 46 were detected by Faraday cup collectors.

A CO_2 working standard (WS) provided the basis for the calculation of $\delta^{13}C$ values for the studied compounds. The IRMS method was programmed such that CO_2 WS pulses were introduced near eluting sample peaks. Several injections of the WS in this manner improve precision in isotope ratio determination. The $\delta^{13}C$ value of the WS gas was (-4.62 ± 0.1)‰, determined through comparison with a reference material (RM) on an IRMS instrument using a dual-inlet analysis. The RM gas had an accurately known $\delta^{13}C_{VPDB}$ value, which is a $\delta^{13}C$ value relative to Vienna Pee Dee Belemnite (V-PDB), the internationally accepted reference standard for stable carbon isotope analysis. All $\delta^{13}C$ values given in this paper are relative to V-PDB.

3 System tests

3.1 VOC reference standard

The system was tested using a VOC standard prepared in a 40 L cylinder at a pressure of 90 bar by injecting known amounts of the VOCs and diluting with synthetic air (99.9996%, Praxair). Although the accuracy of the VOC mixing ratios within the cylinder were limited due to the limited accuracy of syringe injections, the accuracy of the prepared mixture is adequate for conducting instrument tests at known VOC masses and approximating VOC mixing ratios from ambient samples. The VOC standard consisted of isoprene (2-methyl-1,3-butadiene, 99%), MACR (2-methyl-2-propen-1-al, 95%), MVK (1-buten-3-one, 99%), *n*-pentane (98%), benzene (99%), and toluene (99%). The mixing ratios were in the range of 40–60 ppb. However, in contrast to the hydrocarbons, for MVK and MACR the mixing ratios decreased significantly with time. The evaluation of concentration measurements therefore were based on the carbon response of the hydrocarbons. All compounds were obtained from Sigma-Aldrich and used as received. The isotope ratios of aliquots of the compounds were separately analyzed by a conventional combustion, dual-inlet offline IRMS technique.

3.2 Linearity tests

The linearity of the GCC-IRMS instrument was tested using a 5–10 ppmV mixture of isoprene, benzene and toluene prepared inside a 20 L Teflon chamber, using synthetic air as diluent. A fan was placed inside the chamber to ensure complete mixing of the VOCs. The chamber was tested for leaks over a period of 2 h and no significant loss was observed. Teflon ports were installed in one of the walls of the chamber to allow for the introduction of VOCs and synthetic air, and for a sample line to transfer some of the mixture to the GCC-IRMS system. A shut-off valve was used to ensure that the chamber remained closed when not sampling.

Sampling was performed through the use of a six-port switching valve equipped with a 10 mL sample loop. A pump downstream of the six-port valve was used to fill the sample loop with air from the chamber mixture after flushing the transfer lines and the sample loop at a rate of 100 mL min^{-1} for 30 s. Upon valve-switching, the helium carrier gas transferred the 10 mL sample to the already cooled Cryotrap II, bypassing Traps I and II and Cryotrap I. After focusing the VOCs for 5 min, the trap was rapidly heated, releasing the VOCs to the GC.

The concentration of the test mixture was reduced stepwise between GCC-IRMS analyses by withdrawing some of the mixture using a Teflon line and admitting an equal volume of synthetic air to the chamber. In this manner, the height of the chromatographic peaks could be varied over the dynamic range of the IRMS. Tests for determining the precision of the IRMS were carried out using a similar procedure, but without dilution of the sample in between measurements.

4 Measurements of ambient air

4.1 Sampling site

Sampling of ambient air took place during the period of late May to early August 2005 at the Forschungszentrum Jülich, Germany (50°54′31″N, 6°24′45″E). The sampling area lies within a ~4 km^2, mature (~300 year old) mixed deciduous forest area containing tree species such as European oak (*Quercus robur L.*), European beech (*Fagus sylvatica L.*) and silver birch (*Betula pendula Roth.*). Many of the tree species in this forest and in the wider area (e.g. beech, oak, birch) are known to be isoprene emitters. The measurement site lies within a large research centre and the environment is semirural.

4.2 Materials and methods

Ambient samples of 140 L air at ambient pressure were taken from outside the laboratory containing the GCC-IRMS instrumentation using a 1/4″ PTFE transfer line (3 mm ID) connected to the inlet tube of the cryofocussing system. The inlet of the sampling line was placed about 10 m above the ground, 10 m away from several small oak trees. The sampling line was maintained at a temperature of 393 K. A constant flow of NO (19.5 ppmV in N_2, Linde) at 50 mL min^{-1} was introduced into the sample line via a tee piece (8 m upstream of the cryofocussor inlet) when the 800 mL min^{-1} sample flow was drawn into the system. The NO served as a scavenger for background O_3, thus minimizing ozonolysis reactions of the adsorbed hydrocarbons during the 3 h sampling period. This addition of NO is very similar to the methods used by Koppmann et al. (1995), Wedel et al. (1998), and Komenda et al. (2003), and reduces O_3 by ~80% in sample air before entering the adsorption tube of Cryotrap I.

4.3 Data analysis

IRMS and FID traces were digitized and stored, and peaks were evaluated using the MassLynx v4.0i (GV Instruments) software supplied with the IRMS instrument. While the software provided a variety of auto-integration schemes, peak integrations with manual definition of the peak boundaries were performed wherever inappropriate machine integrations were observed. From the integrations of VOC and CO_2 WS peaks in IRMS peak traces for *m/z* 44, 45, and 46, the software routine calculated and reported $\delta^{13}C$ values.

IRMS peak traces were also exported for use with commercial peak-fitting software (Peakfit v4, AISN Software, Inc.). Data files were exported as ASCII files and contained data columns for time (in increments of 0.1 s) and signal intensity in arbitrary units for each of the ion-beam collectors for *m*/z 44, 45, and 46.

The values I_{44}, I_{45}, and I_{46} represent signal intensities of the *m/z* -44, -45, and -46 ion currents for the studied compound. Molecular abundances of CO_2 are generally related to the following compositions of CO_2-isotopologues:

$$I_{44} : \left[{}^{44}\mathrm{CO_2}\right] \propto {}^{12}\mathrm{C}^{16}\mathrm{O}^{16}\mathrm{O} \tag{1}$$

$$I_{45} : \left[{}^{45}\mathrm{CO_2}\right] \propto {}^{13}\mathrm{C}^{16}\mathrm{O}^{16}\mathrm{O} + 2\,{}^{12}\mathrm{C}^{17}\mathrm{O}^{16}\mathrm{O} \tag{2}$$

$$I_{46} : \left[{}^{46}\mathrm{CO_2}\right] \propto {}^{12}\mathrm{C}^{17}\mathrm{O}^{17}\mathrm{O} + 2\,{}^{12}\mathrm{C}^{18}\mathrm{O}^{16}\mathrm{O} + 2\,{}^{13}\mathrm{C}^{17}\mathrm{O}^{16}\mathrm{O} \tag{3}$$

For simplicity ${}^{12}\mathrm{C}^{17}\mathrm{O}^{16}\mathrm{O}+{}^{12}\mathrm{C}^{16}\mathrm{O}^{17}\mathrm{O}$ is written as $2\,{}^{12}\mathrm{C}^{17}\mathrm{O}^{16}\mathrm{O}$ and so on. The target VOC peaks for isoprene, MACR, MVK, *n*-pentane, benzene and toluene in mass traces 44, 45, and 46 were manually fitted to peaks using the Peakfit software. The ASCII data file for each GCC-IRMS analysis was portioned into separate files containing the peaks of interest to reduce computational load and to better fit baselines representative of the peaks under analysis. After opening a truncated IRMS trace in Peakfit, a section of the IRMS trace was prepared for further analysis. The beginning and end of the section was chosen to contain a significant amount of clean baseline data. A logarithmic model was used to fit and subtract the baseline. Figure 5 provides an example of a baseline fit to a section of an IRMS trace.

Five different peak functions were tested for their suitability to fit to peaks in the *m/z*-44 traces of the VOC test mixture. The peak functions were compared for their goodness-of-fit

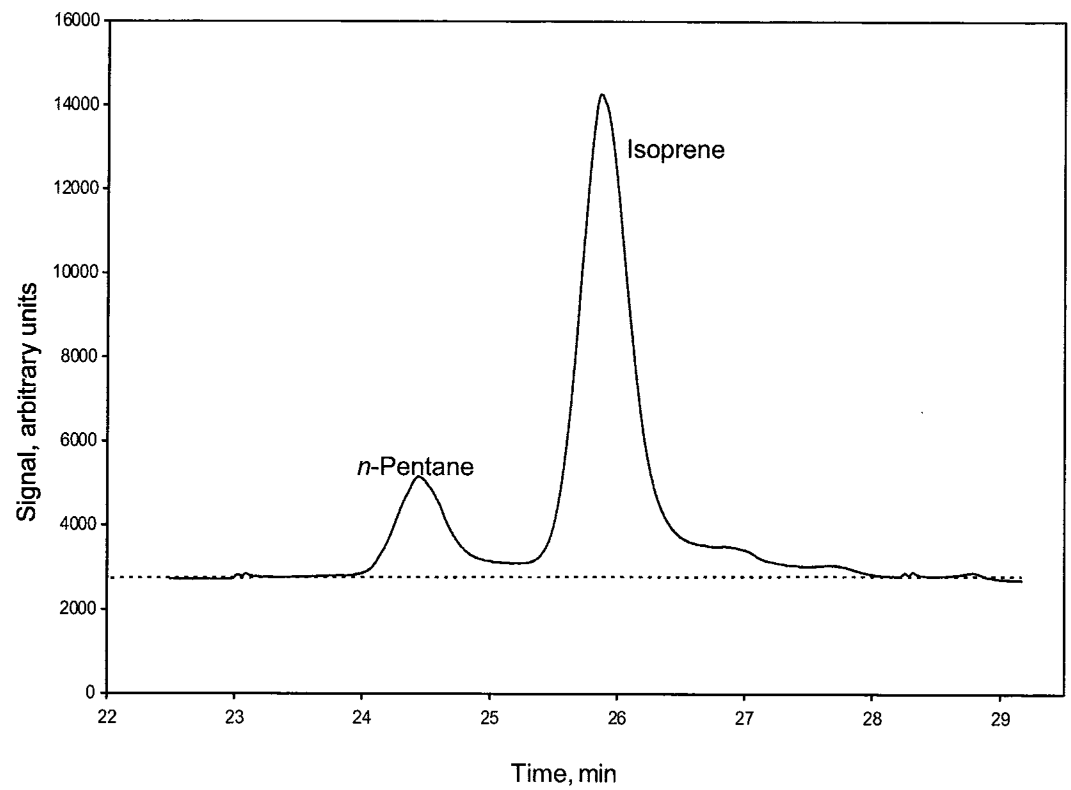

Fig. 5 Baseline fit under *n*-pentane and isoprene peaks from an ambient air sample. A 2nd-derivative logarithmic model was used for the fit The solid line represents the *m/z*-44 IRMS trace and the dotted line is the baseline fit (r^2=0.9979)

to the VOC test-mixture data, which contain target compound peaks for all VOCs to be studied in ambient air samples. The five peak functions were: (1) Haarhoff–Van der Linde (HVL), (2) Exponentially Modified Gaussian (EMG), (3) Half-Gaussian Modified Gaussian (GMG), (4) a five parameter EMG–GMG hybrid (GEMG5), and (5) EMG+GMG. These functions are defined as:

$$\mathrm{HVL}y = \frac{\frac{a_0a_2}{a_1a_3\sqrt{2\pi}}\exp\left(-\frac{1}{2}\left(\frac{x-a_1}{a_2}\right)^2\right)}{\frac{1}{\exp\left(\frac{a_1a_3}{a_2^2}-1\right)}+\frac{1}{2}\left[1+\mathrm{erf}\left(\frac{x-a_1}{\sqrt{2}a_2}\right)\right]} \tag{4}$$

$$\mathrm{EMG}\,y = \frac{a_0}{2a_3}\exp\left(\frac{a_2^2}{2a_3^2}+\frac{a_1-x}{a_3}\right)\left[\mathrm{erf}\left(\frac{x-a_1}{\sqrt{2}a_2}-\frac{a_2}{\sqrt{2}a_3}\right)+\frac{a_3}{|a_3|}\right] \tag{5}$$

$$\mathrm{GMG}\,y = \frac{a_0\exp\left(-\frac{1}{2}\frac{(x-a_1)^2}{a_3^2+a_2^2}\right)\left[1+\mathrm{erf}\left(\frac{a_3(x-a_1)}{\sqrt{2}a_2\sqrt{a_3^2+a_2^2}}\right)\right]}{\sqrt{2\pi}\sqrt{a_3^2+a_2^2}} \tag{6}$$

$$\text{GEMG5}\; y = \frac{a_0 \exp\left(-\frac{1}{2}\frac{\left(a_4 x - a_1 a_4 + a_3^2\right)^2}{a_4^2\left(a_3^2 + a_2^2\right)}\right)}{\sqrt{2\pi}\sqrt{a_3^2 + a_2^2}\, erf\left(\frac{\sqrt{2}a_3}{2a_4} - 1\right)} \times \left[1 + \mathrm{erf}\left(\frac{a_3\left(-a_2^2 + a_4 x - a_1 a_4\right)}{\sqrt{2}a_2 a_4\sqrt{a_3^2 + a_2^2}}\right)\right] \quad (7)$$

$$\text{EMG} + \text{GMG} \quad (8)$$

$$\begin{aligned} y = &\frac{a_0}{4a_3}\exp\left(\frac{2a_1 a_3 - 2a_3 x + a_2^2}{a_3^2}\right) \\ &\times \mathrm{erfc}\left(\frac{a_1 a_3 - a_3 x + a_2^2}{\sqrt{2}a_2 a_3}\right) + \frac{a_0}{2\sqrt{2\pi}\sqrt{a_2^2 + a_4^2}} \\ &\times \exp\left(-\frac{1}{2}\frac{(a_1 - x)^2}{a_2^2 + a_4^2}\right)\mathrm{erfc}\left(\frac{a_4(a_1 - x)}{\sqrt{2}a_2\sqrt{a_2^2 + a_4^2}}\right) \end{aligned}$$

where, in all functions, a_0 is the area, a_1 is the peak center, a_2 is the width of the Gaussian, a_3 and a_4 are distortion factors in the peak model, and, erf and erfc are the error and complementary error functions.

The determination of peak-area values was carried out using the following peak-fitting procedure:

1. *[$^{44}CO_2$].* Fit peaks to *m*/*z*-44 trace, adjusting parameters for every peak such that the resulting set of peaks gives minimal residuals and maximal values for r^2 and F statistics.
2. *[$^{45}CO_2$].* Fit peaks to *m*/*z*-45 trace while retaining similar peak-shape parameters (a_3 and a_4, describing distortion) from Step 1. Retention-time differences between peak-centers determined in Step 1 were maintained here. The residuals trace (depicting differences between sum of fitted peaks and the original trace) for this trace should be similar in shape to that of the *m*/*z*-44 trace.
3. *[$^{46}CO_2$].* Using the same procedure as in Step 2, fit peaks in the *m*/*z*-46 trace.

After fitting all peaks, R45 and R46 values for all target VOC peaks were calculated using:

$$\text{R45} = \left[{}^{45}\text{CO}_2\right] / \left[{}^{44}\text{CO}_2\right] \quad (9)$$

$$\text{R46} = \left[{}^{46}\text{CO}_2\right] / \left[{}^{44}\text{CO}_2\right] \quad (10)$$

Values for the [$^{44}CO_2$], [$^{45}CO_2$], and [$^{46}CO_2$] peaks of the CO_2 WS were obtained by using a summation method (Anderson and Walters 1984), taking the average CO_2 flat-top peak intensity and subtracting the baseline. The average signal 5 s prior to the CO_2 injection was used as a baseline value for this evaluation. The R45 and R46 values for each of the CO_2 WS peaks provide the basis for the calculation of $\delta^{13}C$ values for the studied VOCs. CO_2 WS peaks were measured for their R45 and R46 signal ratios, A method based on that of Santrock et al. (1985) was used for the determination of $\delta^{13}C$ values. This method corrects for the effect of the oxygen isotope ratios $^{17}O/^{16}O$ (R17) and $^{18}O/^{16}O$ (R18) on R45 in order to determine $^{13}C/^{12}C$ R(13). R18 is first calculated using the following equation,

$$3K^2 \cdot \mathrm{R18}^{2a} + 2K \cdot \mathrm{R45} \cdot \mathrm{R18}^a + 2\mathrm{R18} - \mathrm{R46} = 0 \tag{11}$$

Where K and a are constants which describe the relationship between R17 and R18 in the terrestrial oxygen pool. We use the values K=0.0099235 and a=0.516 as given by Santrock et al. (1985) and solve Eq. 11 for R18 using successive approximation. This iterative procedure modifies an initial-guess R18 value until the derivative of Eq. 11 is maximal and both the left and right sides of Eq. 11 show equality. Usually, these conditions are met after four iterations.

R17 and R13 are then obtained using,

$$\mathrm{R17} = K \cdot \mathrm{R18}^a \tag{12}$$

$$\mathrm{R13} = \mathrm{R45} - 2\mathrm{R17} \tag{13}$$

Stable carbon isotope ratios for the sample compound, $\mathrm{R13}_{\mathrm{sample}}$ or $[^{13}C/^{12}C]_{\mathrm{sample}}$, are compared against a working-standard, $[^{13}C/^{12}C]_{\mathrm{WS}}$, value:

$$\delta^{13}C_{\mathrm{sample-WS}} = \left(\frac{[^{13}C/^{12}C]_{\mathrm{sample}} - [^{13}C/^{12}C]_{\mathrm{WS}}}{[^{13}C/^{12}C]_{\mathrm{WS}}}\right) 1,000‰ \tag{14}$$

The $\delta^{13}C$ value of the sample compound is then calculated relative to the absolute ratio of V-PDB, with knowledge of the CO_2 working standard delta value on the V-PDB scale, $\delta^{13}C_{\mathrm{WS-VPDB}}$.

$$\delta^{13}C = \left(\frac{\delta^{13}C_{\mathrm{sample-WS}} \cdot \delta^{13}C_{\mathrm{WS-VPDB}}}{1000‰}\right) + \delta^{13}C_{\mathrm{sample-WS}} + \delta^{13}C_{\mathrm{WS-VPDB}} \tag{15}$$

The $\delta^{13}C_{\mathrm{WS-VPDB}}$ value for Eq. 15 is the stable carbon delta value of the CO_2 working standard.

5 Results and discussion

5.1 Separation of VOCs

The column-switching technique isolated the target VOC peaks isoprene, MACR, MVK, *n*-pentane, benzene and toluene, and discarded nearly all other compounds by directing them to the FID. This technique gave better peak resolution and improved the quality of the peak definitions due to less noisy baselines. Some additional advantages to this setup were the ability to introduce several CO_2 WS gas pulses on a clean background which improved the WS peak shape and the minimization of wear on both the oxidation catalyst and the IRMS detectors from other eluting species.

The coupled IRMS and GC-FID traces of Fig. 6 provide an example of column-switching for an atmospheric sample. Tropospheric CO_2 and most likely also N_2O was partly trapped in the sample concentration system and thus routinely appears in the FID

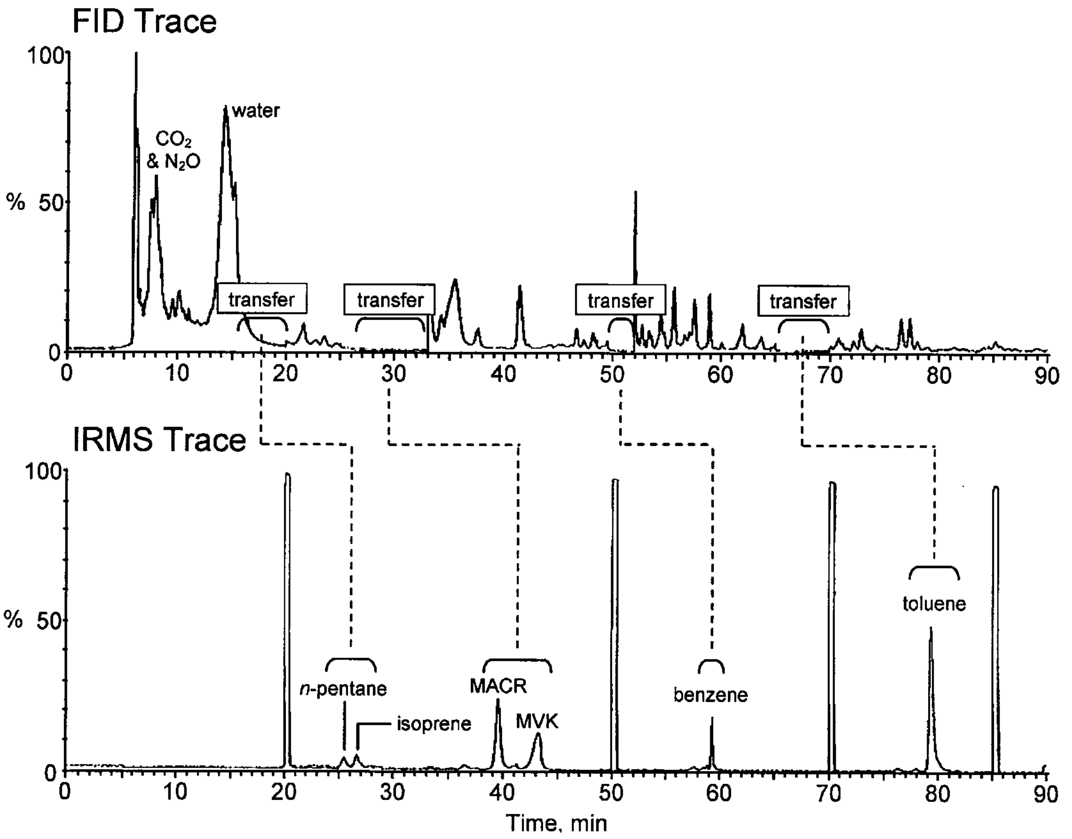

Fig. 6 GC-FID (FID2) and IRMS traces for a 140 L atmospheric sample containing all VOC target compounds. Valve-switching to the Sample→DB-1→BP624→IRMS configuration (from the default Sample→DB-1→FID2 configuration) provided transfer windows for the target VOCs to be separated on a polar column before proceeding to the IRMS. Square peaks in the IRMS trace represent timed CO_2 WS injections through the reference gas injector assembly

trace. It does not, however, interfere with the first target peaks to elute, namely *n*-pentane and isoprene, as it appears 10 min earlier and is completely vented to the FID. Although much of the water vapor in the 140 L samples was condensed and removed in the cryofocussing procedure, a large water peak was still consistently observed in the FID trace 2 min ahead of the column-switching transfer window for the *n*-pentane and isoprene peaks. As a result a portion of the water-peak tail was introduced alongside these target VOCs into the BP624 column. Additional separation on this polar-phase column, however, resulted in complete separation of the water peak from the *n*-pentane peak and all other peaks of interest.

5.2 Peak evaluation

Peaks from the instrument precision tests were evaluated using the MassLynx software and are presented in Table 2. These tests are repeat $\delta^{13}C$ determinations of a prepared mixture of isoprene, MACR and MVK with >1 nA peak heights. The 1σ standard deviation values were in the range of (0.2–0.6)‰ for 10 measurements. A 14.3% decrease in IRMS sensitivity during this measurement period was determined from the relative decrease in average CO_2-WS peak areas and the reported peak areas are corrected for this drift. Further minor changes in VOC peak areas were attributed to chamber loss via small leaks through the chamber wall and adsorption of VOCs to the chamber wall.

Table 2 Reproducibility of GCC-IRMS measurements using MassLynx integration

Run	Isoprene				MACR				MVK			
	Peak height, nA	Corrected area,[a] 10^{-8} A s	Conc., pptV	$\delta^{13}C$, ‰	Peak height, nA	Corrected area,[a] 10^{-8} A s^{-1}	Conc., pptV	$\delta^{13}C$, ‰	Peak height, nA	Corrected area,[a] 10^{-8} A s	Conc., pptV	$\delta^{13}C$, ‰
1	1.61	4.00	342	−26.9	2.70	6.01	514	−24.0	1.90	3.62	310	−27.9
2	1.64	4.16	355	−26.7	3.55	8.04	687	−24.1	3.13	6.14	525	−27.7
3	1.63	4.22	361	−27.9	3.82	8.87	759	−24.6	3.64	7.32	625	−28.2
4	1.60	4.21	360	−27.3	3.99	9.32	796	−24.5	3.89	8.01	684	−27.9
5[b]	1.44	3.77	322	−27.2	4.41	10.1	863	−24.0	4.94	9.98	853	−28.7
6	1.32	3.57	306	−28.3	3.74	9.00	769	−24.5	3.61	7.74	661	−28.1
7	1.29	3.58	306	−27.7	3.82	9.33	797	−24.4	3.88	8.49	725	−28.5
8	1.27	3.59	307	−27.2	3.70	9.34	798	−24.3	3.79	8.55	730	−28.1
9	1.22	3.50	299	−28.3	3.49	8.86	757	−24.5	3.32	7.59	648	−28.5
10	1.17	3.43	293	−27.9	3.35	8.67	741	−24.4	3.16	7.37	629	−28.4
			Mean	−27.5			Mean	−24.3			Mean	−28.2
			S.D.	0.6‰			S.D.	0.2‰			S.D.	0.3‰
			S.E.	0.2‰			S.E.	0.1‰			S.E.	0.1‰

[a] Corrected using change in average CO_2 WS peak areas.

[b] Run 5 performed 17 h after beginning of Run 4.

In the linearity tests for isoprene, benzene and toluene, however, $\delta^{13}C$ values from very small VOC peaks (<1 nA peak height) showed marked differences compared to $\delta^{13}C$ values measured at higher signal response. These deviations are greater than what can be accounted for by counting statistics (Fig. 7). It was suspected that this is caused by interference from

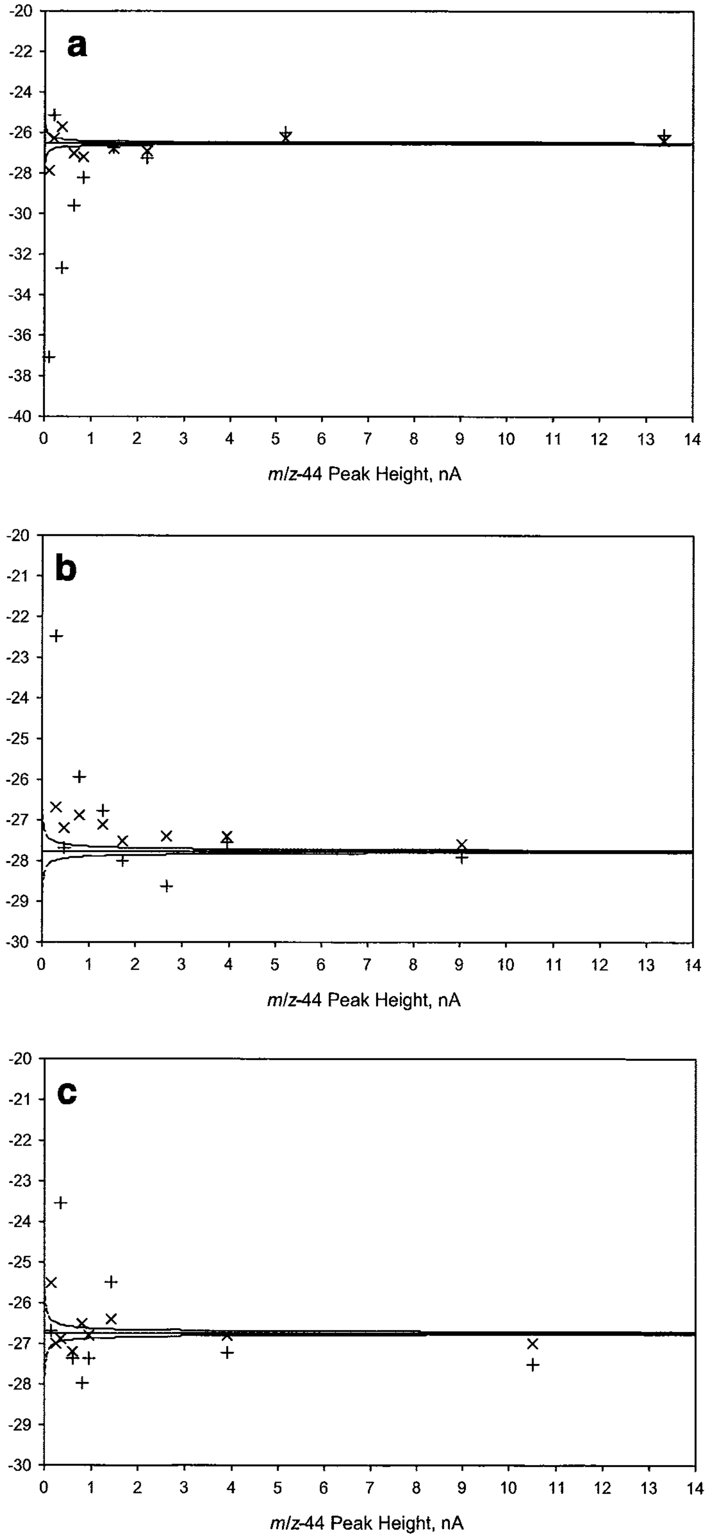

Fig. 7 Stable carbon delta values as a function of peak height (in nA) from GCC-IRMS linearity tests using a VOC test mixture incrementally diluted with synthetic air. $\delta^{13}C$ determinations for isoprene, benzene, and toluene (graphs **a**, **b**, and **c**, respectively) were carried out by MassLynx v4.0i integration (+) and the EMG+GMG peak-fitting method (×). *Center lines* are average $\delta^{13}C$ values for MassLynx integrations at *m*/*z*-44 peak heights greater than 1 nA. *Outer lines* represent estimated uncertainty in $\delta^{13}C$ resulting from IRMS-detector counting statistics

nearby impurity peaks and unrealistic baseline and peak-boundary definitions during the integration procedure. Although the MassLynx software allows the user to set a variety of integration parameters, this problem could not be eliminated using the MassLynx software for signal levels below ~1 nA.

Using several GC-IRMS traces of the 80 L VOC test mixture containing ~50 ppbV each of *n*-pentane, isoprene, MACR, MVK, benzene, and toluene, five peak functions available in the Peakfit software (HVL, EMG, GMG, GEMG5 and EMG+GMG, see 4.3) were evaluated for both goodness-of-fit to VOC peaks and precision of VOC $\delta^{13}C$ values. Values for the r^2 and F statistics were estimated for each of the peak functions and are presented in Table 3; an example peak-fit is provided in Fig. 8. Positive residuals are often observed indicating that the fitting of the peak gives an underestimate of the true peak area. Many of the observed positive residuals occur from poor fitting to the peak tailing. Dead volumes due to capillary connections, changes in capillary diameter, open-splits, and residence time in the IRMS source all contribute toward broadening and tailing peaks. Nevertheless, these residuals are small compared to the VOC peak heights and manifest themselves in all three IRMS traces (*m/z* 44, 45, and 46), and thus have a low impact on the calculated $\delta^{13}C$ values.

The modified Gaussian functions gave more accurate peak shapes than the HVL function. The HVL, GMG and GEMG5 functions did not consistently fit the observed peaks and thus gave poorer values for r^2 and F than did EMG and EMG+GMG. The EMG and EMG+GMG functions gave the best fits and resulted in r^2 and F statistics that were uniformly high for all peaks.

Table 4 presents a comparison between offline $\delta^{13}C$ values and online $\delta^{13}C$ values using different peak fits. Bias from offline $\delta^{13}C$ values is especially marked for the HVL and GEMG5 fits. HVL and GEMG5 had average 1σ standard deviations of 3.4‰ and 1.6‰, respectively, while the EMG function, which otherwise yielded good fitting statistics had an average S.D. of 1.7‰. The GMG and EMG+GMG functions showed the least average S. D. for the $\delta^{13}C$ values: 0.5‰ and 0.6‰.

Peak heights for MACR and MVK were extremely low (0.02–0.10 nA) due to loss of these VOCs within the pressurized 80 L cylinder. This loss may change the $\delta^{13}C$ values of

Table 3 Summary of goodness-of-fit statistics from the use of five different peak functions on several IRMS traces of the VOC test mixture (Average results from fits to several runs of the VOC test mixture; uncertainties are given at the 1σ level of significance.)

Peak function	Target VOCs in section of IRMS trace							
	n-pentane, isoprene		MACR, MVK		Benzene		Toluene	
	r^2	F	r^2	F	r^2	F	r^2	F
HVL	0.9934± 0.0016	68,657± 8,709	0.9846± 0.0038	14,496± 868	0.9927± 0.0008	123,393± 32,059	0.9925± 0.0009	109,069± 13,691
EMG	0.9967± 0.0011	151,222± 23,367	0.9904± 0.0072	29,220± 14,870	0.9968± 0.0001	275,521± 40,151	0.9960± 0.0006	209,130± 32,051
GMG	0.9950± 0.0012	90,518± 12,618	0.9846± 0.0058	14,793± 1,127	0.9944± 0.0009	163,132± 50,864	0.9938± 0.0008	133,079± 16,849
GEMG5	0.9957± 0.0013	85,628± 13,167	0.9873± 0.0068	15,131± 3,936	0.9952± 0.0008	143,442± 46,813	0.9950± 0.0004	121,787± 8,670
EMG +GMG	0.9972± 0.0008	130,632± 21,189	0.9896± 0.0075	20,895± 10,053	0.9972± 0.0010	258,087± 12,642	0.9974± 0.0007	261,308± 71,226

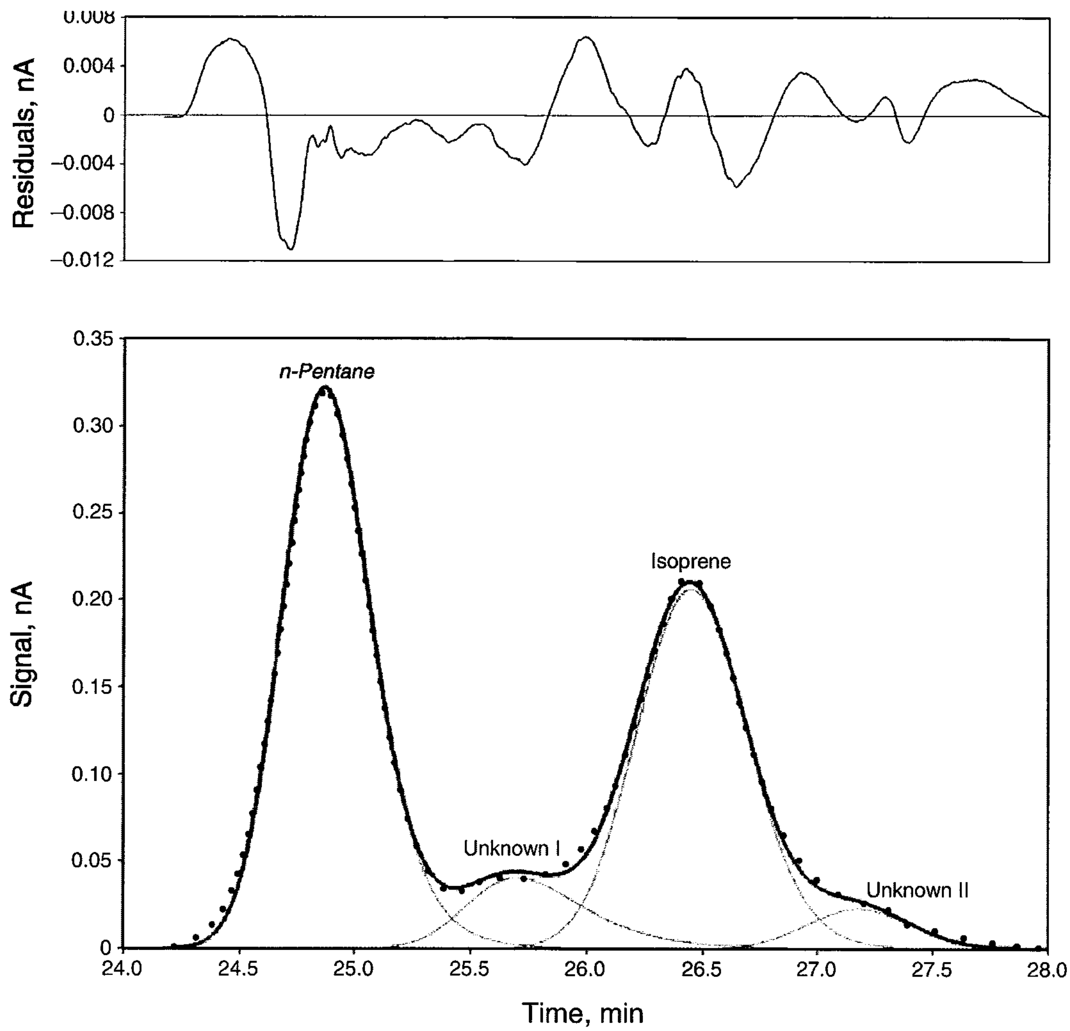

Fig. 8 Result of peak-fitting to *n*-pentane, isoprene, and 2 unknown peaks using the EMG+GMG function. The *dotted line* represents the *m/z*-44 signal, the *grey lines* are the fitted peak functions, and the *solid black line* represents the sum of the fitted peaks. Residuals, the difference between the sum of fitted peaks and the original trace, are plotted separately above. The r^2 and F values for this fit are 0.9985 and 83060, respectively

MACR and MVK within the cylinder. The results, however, do not show significantly more bias from offline $\delta^{13}C$ values compared to other VOCs with much greater signal response. Fitted peaks for MACR, for example, differed by ±(2.1–2.7)‰ (EMG+GMG) and ±(1.8–1.9)‰ (EMG) from the offline $\delta^{13}C$ values.

Peak fitting was used to estimate $\delta^{13}C$ values for a range of IRMS signal intensities. Figure 7 provides a comparison of $\delta^{13}C$ determinations from MassLynx integration and EMG+GMG peak evaluation for isoprene, benzene, and toluene. Fitting peaks using EMG+GMG gave $\delta^{13}C$ values with least amount of bias at low signal levels (<1 nA).

Because of the combination of high goodness-of-fit statistics and accuracy in evaluations of $\delta^{13}C$, subsequent peak-fitting for ambient samples was performed using solely the EMG+GMG function. Uncertainty estimates for $\delta^{13}C$ values using the EMG+GMG peak-fitting procedure were determined for several peak-height ranges using average standard deviation values from the linearity tests (Table 5). These uncertainties are estimated from tests using prepared VOC mixtures. Therefore, GCC-IRMS analyses of ambient samples in cases

Table 4 Difference between $\delta^{13}C$ values by GCC-IRMS and offline IRMS. GCC-IRMS results are shown for different peak fitting algorithms

VOC	Offline $\delta^{13}C$, ‰	m/z-44 peak height, nA	HVL $\Delta\delta^{13}C$, ‰	EMG $\Delta\delta^{13}C$, ‰	GMG $\Delta\delta^{13}C$, ‰	GEMG5 $\Delta\delta^{13}C$, ‰	EMG+GMG $\Delta\delta^{13}C$, ‰
n-Pentane	−30.0±0.1	3.5	−3.4	−3.2	−1.7	−0.5	−0.6
		4.0	2.6	−1.4	1.4	−1.5	−2.9
		2.4	4.4	−1.4	1.1	2.4	−0.9
		2.3	2.5	2.1	1.3	2.9	0.7
		2.4	2.4	−2.3	0.7	−0.8	−1.4
		2.8	−1.7	−1.5	−1.1	−1.5	−0.5
Isoprene	−25.1±0.1	11.7	−1.6	−0.2	−0.1	−1.6	−1.2
		13.0	−1.9	0.5	−1.1	−3.8	0.7
		6.8	3.9	−0.3	1.1	5.0	0.4
		6.8	4.7	0.4	−0.3	3.2	1.2
		7.0	−4.4	2.1	−0.4	2.9	1.0
		7.6	−1.7	−0.8	−0.5	−1.6	−0.9
MACR	−28.7±0.1	0.1	6.0	1.4	−0.1	−2.2	0.5
		0.06	−3.9	−3.2	1.9	−3.3	−0.9
MVK	−30.8±0.3	0.02	5.2	−2.1	2.4	−2.0	2.6
		0.02	−2.7	2.6	2.3	3.1	3.2
Benzene	−27.2±0.1	9.4	4.4	−2.4	−0.6	−3.9	0.5
		10.0	−1.6	−0.9	0.4	−1.3	−1.1
Toluene	−26.8±0.2	4.2	3.4	2.8	−0.9	−2.3	−1.0
		5.1	2.6	−0.7	−1.3	1.1	−1.1
		4.4	3.6	−1.3	−1.0	−1.3	−1.1

where the peak-fitting determination of $\delta^{13}C$ is highly sensitive to peaks adjacent to the target VOC can be significantly higher at peak heights <1 nA.

5.3 Ambient samples

Mixing ratios and $\delta^{13}C$ values for VOCs from two daytime measurement periods are tabulated in Table 6. The mixing ratios of the primarily man made VOCs *n*-pentane,

Table 5 Reproducibilities for EMG+GMG peak-fitting at different peak-height ranges

m/z-44 peak height, nA	m/z-44 peak area, 10^{-8} A s	Sample mass, ng C	Number of data points	Mixing ratio, pptV[a]	Reproducibility of $\delta^{13}C$ value, ‰	Bias, ‰[b]	$\delta^{13}C_{\mathrm{Count.Stat.}}$, ‰[c]
1.0–14	2.2–35	1.8–25	12	190–3,000	±0.3	–	0.03–0.12
0.5–1.0	1.0–2.2	0.9–1.8	6	85–190	±0.5	0.03	0.12–0.17
0.25–0.5	0.6–1.0	0.4–0.9	3	50–85	±0.6	−1.29	0.17–0.24
0.05–0.25	0.1–0.6	0.1–0.4	4	10–50	±0.8	0.26	0.24–0.55

[a] Based on a 140 L sample of air.

[b] Difference between mean values for $\delta^{13}C$ with PH>1.0 nA and $\delta^{13}C$ values of the corresponding peak height range.

[c] Uncertainty in $\delta^{13}C$ value due to counting statistics: $\delta^{13}C_{\mathrm{Count.Stat}} = \left(\frac{0.0107 I_{44}}{10^9 e}\right)^{-0.5} \times 1,000‰$

where I_{44} represents the IRMS signal intensity at the mass-44 detector (in nA units), *e* is the elementary charge (1.602×10^{-19} A·s), and 0.0107 is the conversion from m/z-44 to m/z-45 ions (i.e. using the natural abundance of ^{13}C isotopes).

Table 6 Mixing ratios and $\delta^{13}C$ values for VOCs in air samples taken at Forschungszentrum Jülich, Germany (Sample volume was 140 L for all measurements.)

Date/time of measurement	*n*-Pentane		Isoprene		MACR		MVK		Benzene		Toluene	
	$\delta^{13}C$, ‰	Conc., pptV	$\delta^{13}C$, ‰	Conc., pptV	$\delta^{13}C$, ‰	Conc., pptV	$\delta^{13}C$, ‰	Conc., pptV	$\delta^{13}C$, ‰	Conc., pptV	$\delta^{13}C$, ‰	Conc., pptV
07.13.05												
10:15–13:15	−29.1	34	−19.0	48	−17.7	32	−14.9	73	−23.5	94	−25.2	155
13:45–16:45	−24.9	27	−21.1	127	−21.1	57	−20.7	110	−25.1	98	−23.9	68
17:15–20:15	−16.2	12	−25.4	90	−21.0	15	−28.5	47	−24.4	24	−26.3	44
07.18.05												
11:05–14:05	−23.0	95	−23.8	46	−28.9	195	–	197	−28.8	388	–	1046
14:35–17:35	−22.8	42	−22.3	219	−22.4	164	−15.2	279	−26.2	391	−18.0	675
18:00–21:00	–	31	–	21	−19.0	113	–	190	−29.4	147	−24.2	370

benzene, and toluene, range from 10 pptV to approximately 1 ppbV, which is consistent with a semirural location. The isoprene, MVK, and MACR mixing ratios are in the mid pptV range, compatible with the location of the measurement site in the vicinity of forests. The MVK over MACR concentration ratios have an average of approximately 2, similar to daytime measurements near sources of isoprene (Stroud et al. 2001; Apel et al. 2002). This suggests that MVK and MACR in these measurements are primarily products of the atmospheric oxidation of isoprene. However, it should be noted that in our measurements the MVK and MACR mixing ratios are of comparable magnitude, in some cases even higher, than those of isoprene. This accumulation of isoprene oxidation products strongly suggests that isoprene in the sampled air masses has been subject to substantial atmospheric processing.

It has been shown that changes in the stable carbon isotope ratios can be used as indicators for atmospheric processing of VOC (Rudolph and Czuba 2000). The $\delta^{13}C$ values of isoprene emitted from C3 plants are typically in the range from −26‰ to −29‰ (Rudolph et al. 2003). Similar isotope ratios between −27‰ and −29‰ have been found for emissions of *n*-pentane, benzene and toluene from major anthropogenic sources (Rudolph et al. 2002). In the atmosphere oxidation reactions generally will result in an enrichment of ^{13}C in the VOCs (Rudolph et al. 2000) and the $\delta^{13}C$ values will increase. The magnitude of the change depends on the reactivity of the compounds, the kinetic isotope effect for the reaction, the time between emission and observation, and the average reactant concentration. However, atmospheric mixing processes and variations in emission rates have little direct impact on the $\delta^{13}C$ values. Consequently there is no easily predictable dependence between $\delta^{13}C$ values and mixing ratios of VOCs. Moreover, the spatial and temporal scales of the processes which determine VOC mixing ratios and $\delta^{13}C$ values depend on the reactivity of the individual compound.

For reactive VOCs with short atmospheric residence times, such as isoprene, mixing ratios and $\delta^{13}C$ values will be primarily determined by local processes. The finding that the $\delta^{13}C$ values of isoprene in Table 6 are on average well above those of emissions (Rudolph et al. 2003) agrees with the finding that isoprene oxidation products must have been accumulated in the samples air masses.

Similar to the $\delta^{13}C$ values of isoprene, the $\delta^{13}C$ values of reactive man made VOCs, *n*-pentane and toluene, are generally higher than the $\delta^{13}C$ values of their sources (Rudolph et al.

2002, 2003), in a few cases of comparable magnitude, but never significantly lower. This is compatible with the concept that atmospheric processing is a major contribution to the variability of the $\delta^{13}C$ values of atmospheric VOCs. The absence of a clear dependence between mixing ratio and $\delta^{13}C$ values demonstrates that for *n*-pentane, isoprene, and toluene the atmospheric mixing ratios found here are predominantly determined by the strength of emissions and atmospheric mixing and only to a lesser extent by atmospheric removal.

For less reactive VOCs (e.g. benzene), regional and large scale processes may be far more important, especially under conditions where the influence of local sources is small. On July 18th (Table 6) the benzene mixing ratios are several hundred pptV and the corresponding $\delta^{13}C$ values range around −28‰, which is identical to the stable carbon isotope ratios of benzene emissions (Rudolph et al. 2002). This indicates that these benzene mixing ratios are dominated by local or regional emissions, which have been subject to only a marginal extent of processing. In contrast to this on July 13th the benzene $\delta^{13}C$ values are significantly higher than the isotope ratios of benzene emissions, which indicates substantial atmospheric processing of benzene. Due to the low reactivity this requires that the benzene mixing ratios are dominated by long range transport, which is consistent with the low benzene mixing ratios observed on July 13th.

On average the $\delta^{13}C$ values of MVK and MACR in Table 6 are well above the stable carbon isotope ratios of isoprene emissions. Qualitatively this is compatible with the concept that MVK and MACR have been accumulated in the sampled air mass after being formed by atmospheric oxidation of isoprene. However, presently there is no published quantitative information on the isotope fractionation associated with the formation of MVK and MACR from isoprene or the kinetic isotope effects for their atmospheric loss reactions. Consequently, at this time any interpretation of MVK or MACR isotope ratios is tentative.

6 Summary and conclusions

A GCC-IRMS technique was successfully developed to measure stable carbon isotope ratios of light VOCs. The combination of enrichment from large sample volumes, two-column GC separation, and a peak-fitting technique allowed for the detection and quantification of $\delta^{13}C$ values for isoprene, MACR, MVK, benzene and toluene in ambient air at pptV levels. The measurements carried out with this technique clearly demonstrates the usefulness of isotope ratio measurements for studies of the chemistry of atmospheric VOCs. Specifically, the ability to measure the stable carbon isotope ratios of MVK and MACR is very promising for gaining further insight into the atmospheric oxidation of isoprene, although presently the lack of laboratory studies of the isotope fractionation effects for the formation and removal of reactions of MVK and MACR prevents quantitative interpretation of such measurements.

The presented instrumentation and method can easily be modified for measurements of a wide range of other atmospheric VOCs and isotope ratios other than $^{12}C/^{13}C$, such as H/D. The main limitation of the presented method is the lack of tested procedures for field sampling and storage of large volumes of air for later analysis of isotope ratios in the laboratory.

References

Anderson, D.J., Walters, R.R.: Effect of baseline errors on the calculation of statistical moments of tailed chromatographic peaks. J. Chromatogr. Sci. **22**, 353–359 (1984)

Anderson, R.S., Czuba, E., Ernst, D., Huang, L., Thompson, A.E., Rudolph, J.: Method for measuring carbon kinetic isotope effects of gas-phase reactions of light hydrocarbons with the hydroxyl radical. J. Phys. Chem. A **107**, 6191–6199 (2003)

Apel, E.C., Riemer, D.D., Hills, A., Baugh, W., Orlando, J., Faloona, I., Tan, D., Brune, W., Lamb, B., Westberg, H., Carroll, M.A., Thornberry, T., Geron, C.D.: Measurement and interpretation of isoprene fluxes and isoprene, methacrolein, and methyl vinyl ketone mixing ratios at the PROPHET site during the 1998 Intensive. J. Geophys. Res. **107**, 4034 (2002), DOI 10.1029/2000JD000225

Atkinson, R.: Gas-phase tropospheric chemistry of volatile organic compounds. 1. Alkanes and alkenes. J. Phys. Chem. Ref. Data **26**, 215–290 (1997)

Atkinson, R.: Atmospheric chemistry of VOCs and NO_x. Atmos. Environ. **34**, 2063–2101 (2000)

Atkinson, R., Arey, J.: Atmospheric chemistry of biogenic organic compounds. Acc. Chem. Res. **31**, 574–583 (1998)

Atkinson, R., Arey, J.: Atmospheric degradation of volatile organic compounds. Chem. Rev. **103**, 4605–4638 (2003)

Bandowe, B. Developement and application of an analytical method to measure oxygenated volatile organic compounds (OVOCs) in the atmosphere, Master Thesis, Technische Universität. Braunschweig 2005

Biesenthal, T.A., Wu, Q., Shepson, P.B., Wiebe, H.A., Anlauf, K.G., Mackay, G.I.: A study of relationships between isoprene, its oxidation products, and ozone, in the lower Fraser Valley, BC. Atmos. Environ. **31**, 2049–2058 (1997)

Bill, M., Rhew, R.C., Weiss, R.F., Goldstein, A.H.: Carbon isotope ratios of methyl bromide and methyl chloride emitted from a coastal salt marsh. Geophys. Res. Lett. **29** (2002), DOI 10.1029/2001GL012946

Bill, M., Conrad, M.E., Goldstein, A.H.: Stable carbon isotope composition of atmospheric methyl bromide. Geophys. Res. Lett. **31**, L04109 (2004), DOI 10.1029/2003GL018639

Claeys, M., Graham, B., Vas, G., Wang, W., Vermeylen, R., Pashynska, V., Cafmeyer, J., Guyon, P., Andreae, M.O., Artaxo, P., Maenhaut, W.: Formation of secondary organic aerosols through photooxidation of isoprene. Science **303**, 1173–1176 (2004)

Guenther, A., Hewitt, C.N., Erickson, D., Fall, R., Geron, C., Graedel, T., Harley, P., Klinger, L., Lerdau, M., McKay, W.A., Pierce, T., Scholes, B., Steinbrecher, R., Tallamraju, R., Taylor, J., Zimmerman, P.: A global model of natural volatile organic compound emissions. J. Geophys. Res. **100**, 8873–8892 (1995)

Kesselmeier, J., Staudt, M.: Biogenic volatile organic compounds (VOC): An overview on emission, physiology and ecology. J. Atmos. Chem. **33**, 23–88 (1999)

Komatsu, D.D., Tsunogai, U., Yamaguchi, J., Nakagawa, F.: A selective unsaturated hydrocarbon subtraction technique for stable carbon isotopic analysis of atmospheric methyl chloride, methyl bromide, and C_2–C_5 saturated hydrocarbons using continuous-flow isotope ratio mass spectrometry. Rapid. Commun. Mass Spectrom. **19**, 477–483 (2005)

Komenda, M., Schaub, A., Koppmann, R.: Description and characterization of an on-line system for long-term measurements of isoprene, methyl vinyl ketone, and methacrolein in ambient air. J. Chromatogr. A **995**, 185–201 (2003)

Koppmann, R., Johnen, F.J., Khedim, A., Rudolph, J., Wedel, A., Wiards, B.: The influence of ozone on light nonmethane hydrocarbons during cryogenic preconcentration. J. Geophys. Res. **100**, 11383–11392 (1995)

Lee, Y.-N., Zhou, X., Kleinman, L.I., Nunnermacker, L.J., Springston, S.R., Daum, P.H., Newman, L., Keigley, W.G., Holdren, M.W., Spicer, C.W., Young, V., Fu, B., Parrish, D.D., Holloway, J., Williams, J., Roberts, J.M., Ryerson, T.B., Fehsenfeld, F.C.: Atmospheric chemistry and distribution of formaldehyde and several multioxygenated carbonyl compounds during the 1995 Nashville/Middle Tennessee Ozone Study. J. Geophys. Res. **103**, 22449–22462 (1998)

Levis, S., Wiedinmyer, C., Bonan, G.B., Guenther, A.: Simulating biogenic volatile organic compound emissions in the community climate system model. J. Geophys. Res. **108**, 4659 (2003), DOI 10.1029/2002JD003203

McKeen, S.A., Liu, S.C.: Hydrocarbon ratios and photochemical history of air masses. Geophys. Res. Lett. **20**, 2363–2366 (1993)

Monson, R.K., Holland, E.A.: Biospheric trace gas fluxes and their control over tropospheric chemistry. Annu. Rev. Ecol. Syst. **32**, 547–576 (2001)

Montzka, S.A., Trainer, M., Angevine, W.M., Fehsenfeld, F.C.: Measurements of 3-methyl furan, methyl vinyl ketone, and methacrolein at a rural forested site in the southeastern United States. J. Geophys. Res. **100**, 11393–11402 (1995)

Pierotti, D., Wofsy, S.C., Jacob, D., Rasmussen, R.A.: Isoprene and its oxidation products: methacrolein and methyl vinyl ketone. J. Geophys. Res. **95**, 1871–1881 (1990)

Poisson, N., Kanakidou, M., Crutzen, P.J.: Impact of nonmethanehydrocarbons on tropospheric chemistry and the oxidizing power of the global troposphere: 3-dimensional modelling results. J. Atmos. Chem. **36**, 157–230 (2000)

Rudolph, J., Czuba, E.: On the use of isotopic composition measurement of volatile organic compounds to determine the "photochemical age" of an air mass. Geophys. Res. Lett. **27**, 3865–3868 (2000)

Rudolph, J., Lowe, D.C., Martin, R.J., Clarkson, T.S.: A novel method for compound specific determination of δ13C in volatile organic compounds at ppt levels in ambient air. Geophys. Res. Lett. **24**, 659–662 (1997)

Rudolph, J., Czuba, E., Huang, L.: The stable carbon isotope fractionation for reactions of selected hydrocarbons with OH-radicals and its relevance for atmospheric chemistry. J. Geophys. Res. **105**, 29329–29346 (2000)

Rudolph, J., Czuba, E., Norman, A.L., Huang, L., Ernst, D.: Stable carbon isotope composition of nonmethane hydrocarbons in emissions from transportation related sources and atmospheric observations in an urban atmosphere. Atmos. Environ. **36**, 1173–1181 (2002)

Rudolph, J., Anderson, R.S., Czapiewski, K.v., Czuba, E., Ernst, D., Gillespie, T., Huang, L., Rigby, C., Thompson, A.E.: The stable carbon isotope ratio of biogenic emissions of isoprene and the potential use of stable isotope ratio measurements to study photochemical processing of isoprene in the atmosphere. J. Atmos. Chem. **44**, 39–55 (2003)

Saito, T., Tsunogai, U., Kawamura, K., Nakatsuka, T., Yoshida, N.: Stable carbon isotopic composition of light hydrocarbons over the western North Pacific and implications for their photochemical ages. J. Geophys. Res. **107** (2002) 10.1029/2000JD000127.

Santrock, J., Studley, S.A., Hayes, J.M.: Isotopic analyses based on the mass spectrum of carbon dioxide. Anal. Chem. **57**, 1444–1448 (1985)

Stroud, C.A., Roberts, J.M., Goldan, P.D., Kuster, W.C., Murphy, P.C., Williams, E.J., Hereid, D., Parrish, D., Sueper, D., Trainer, M., Fehsenfeld, F.C., Apel, E.C., Riemer, D., Wert, B., Henry, B., Fried, A., Martinez-Harder, M., Harder, H., Brune, W.H., Li, G., Xie, H., Young, V.L.: Isoprene and its oxidation products, methacrolein and methylvinyl ketone, at an urban forested site during the 1999 Southern Oxidants Study. J. Geophys. Res. **106**, 8035–8046 (2001)

Thompson, A.E.: Stable carbon isotope ratios of nonmethane hydrocarbons and halocarbons in the atmosphere, Dissertation, York University (2003)

Tsunogai, U., Yoshida, N., Gamo, T.: Carbon isotopic compositions of C_2–C_5 hydrocarbons and methyl chloride in urban, coastal and marine atmospheres over the western North Pacific. J. Geophys. Res. **104**, 16033–16039 (1999)

Warneke, C., Holzinger, R., Hansel, A., Jordan, A., Lindinger, W., Pöschl, U., Williams, J., Hoor, P., Fischer, H., Crutzen, P.J., Scheeren, H.A., Lelieveld, J.: Isoprene and its oxidation products methyl vinyl ketone, methacrolein, and isoprene related peroxides measured online over the tropical rain forest of Surinam in March 1998. J. Atmos. Chem. **38**, 167–185 (2001)

Wedel, A., Müller, K.P., Ratte, M., Rudolph, J.: Measurements of volatile organic compounds (VOC) during POPCORN 1994: applying a new on-line GC-MS-technique. J. Atmos. Chem. **31**, 73–103 (1998)

Wiedinmyer, C., Friedfeld, S., Baugh, W., Greenberg, J., Guenther, A., Fraser, M., Allen, D.: Measurement and analysis of atmospheric concentrations of isoprene and its reaction products in central Texas. Atmos. Environ. **35**, 1001–1013 (2001)